MANTECH Publications
Journal of Material Science & Manufacturing Technology
Volume 4 Issue 2

Finite Element Analysis of Weld Bead Geometry of Micro Plasma Arc Welding Titanium (Ti-6Al-4V) Alloy

Posimsetti Hanuma*, Dr. Kondapalli Siva Prasad**
Student, Professor***
Department of Mechanical Engineering
Anil Neerukonda institute of Technology and Sciences, Visakhapatnam, India
Corresponding author's email id:*hanumanaidu084@gmail.com,kspanits@gmail.com*
DOI: http://doi.org/10.5281/zenodo.3373127

Abstract

Precision welding is a key step in the manufacturing of thin walled metal bellows, diaphragms, sensors etc. and for this; a welding process must reliably maintain tight operational tolerance without interfering with product function. The present work is focused on pulsed current Micro Plasma Arc Welding (MPAW) welding of Titanium (Ti-6Al-4V) metal. Peak current, back current, Pulse rate and Pulse width are chosen as welding parameters, whereas Front width and Back width of the weld bead are considered as output responses. Finite Element Analysis (FEA) is done in ANSYS workbench R15.0 at different peak currents keeping base current, pulse rate and pulse width constant. The values of front width and back width obtained experimentally and FEA are compared and % error is found.

Keywords: *Plasma arc welding, FEA analysis, welding parameters, titanium (ti-6Al-4V).*

INTRODUCTION

Ti-6Al-4V (Ti-64) is one of the most important titanium alloys. It accounts for about 45% of the total weight of all titanium alloys produced and more than 80% of titanium alloys used in aerospace industry. Ti-64 is also used in medical implants and in automotive, marine and chemical industries. Ti-64 is and α+β alloy which combines attractive mechanical properties with good workability and the best weld ability of α+β alloys.[2]

Application of Ti-64 is limited to about 350°C which limits its use in high temperature applications. In the aerospace industry, Ti-64 is extensively used in the cold section of jet engines, i.e. in the fan and compressor sections. For successful welding of titanium, some factors need to be considered. Titanium is extremely reactive in temperatures exceeding 500-650°C. It reacts with elements in impurities or air such as C, O, N, and H. These elements strengthen titanium but small amounts also impair ductility and toughness of titanium joints. The effects of the heating and cooling cycles involved in welding processes on the mechanical properties of the alloys and the specific alloy composition also need to be considered. PAW process is one of the best welding methods available for joining titanium and its alloys.[33].

Abhishek B P et al. [12] investigated the behavior of welded zone is affected by variation in temperature distributions, microstructures and mechanical properties of the materials.The main objectives of this simulation is the determination of temperatures and stresses during and after the process. Temperature distributions define the heat affected zone (HAZ) where materials properties are affected.Edwin Raja Dhas, J.a et al. [13] investigated the modeling and prediction of dimensions of Heat-Affected Zone for SAW process using Finite Element Analysis (FEA) and Artificial Neural Network (ANN).V Dhinakaran, N Siva Shanmugam et al. [14] analyzed the Numerical simulations are carried out with the proposed parabolic Gaussian heat source (PGHS) model.[3]Experimental trials on thin titanium alloy sheets are carried out to enable the validation of the proposed PGHS model and appears to have a good correlation with the experimental result and clear parabolic shape of the bead.

C.S. Wu et al. [15] examined the available heat source models, either planar one like Gaussian or body ones like double-ellipsoidal and rotary Gaussian modes. This adaptive heat source model, finite-element analysis of temperature profile in keyhole PAW is conducted and the weld geometry is determined.PrashantSagar et al. [16] studied the TIG welding and main focus is on temperature distribution. The aim of the study presented in this paper is to determine the temperature distribution profile by using effective and reliable method of simulation. [33] Simulation was performed for Titanium-G5 alloy (Ti-6Al-4V), the most commonly used alloy of titanium.Sadaf Batool, Mushtaq Khan et al. [17] focuses on comparison of the weld

geometry, distortion, microstructure and mechanical properties of thin SS 304L sheets welded using micro-plasma arc welding and tungsten inert gas welding process.Tao Zhang et al. [18] studied the three-dimensional transient model is established to analyze numerically the evolution of the weld pool, the keyhole shape and dimensions, and the fluid convection and temperature profiles in a PAW weld pool.

The dynamic development of keyhole geometry and its interaction with the weld pool are numerically simulated.Hafiz Waqar Ahmad et al.[19] studied welding residual stresses of multi-pass dissimilar material welded joint between alloy 617 and 12Cr steel were analyzed numerically and experimentally.

In any welded joint the quality of weld bead is a primary objective. The deposited filler metal on and in the work surface when the wire or electrode is melted and fusion in to the steel is called bead. There are two types of beads are available, (a) narrow bead (b) wave bead.A stringer bead is a narrow bead with only a dragging Motion Or Light Oscillation, while a wave bead is a wider width more Oscillation. [26].

The objective of the paper to compare the experimental values of front width and back width of the weld bead with FEA values and compute the % error.

EXPERMENTATION

Plasma arc welding, the plasma is generated between tungsten electrode and the nozzle ,this plasma provides the heat required for melting the faying surfaces and get the metallic continuity without adding any filler material[26].Among the welding methods available for joining titanium and its alloys in aerospace industry, plasma arc welding (PAW) has the ability to produce high depth-to-width ratio and higher welding rate, and hence, PAW is preferred in comparison with other conventional arc welding methods for welding titanium and its alloys[35].

In plasma arc welding (PAW), introduced around 1960, a tungsten electrode is contained in a specially designed nozzle that focuses a high-velocity stream of inert gas (e.g. argon or argon–hydrogen mixtures) into the region of the arc to form a high-velocity, intensely hot (25,000°C) plasma arc stream [35], as shown in Fig. 1.

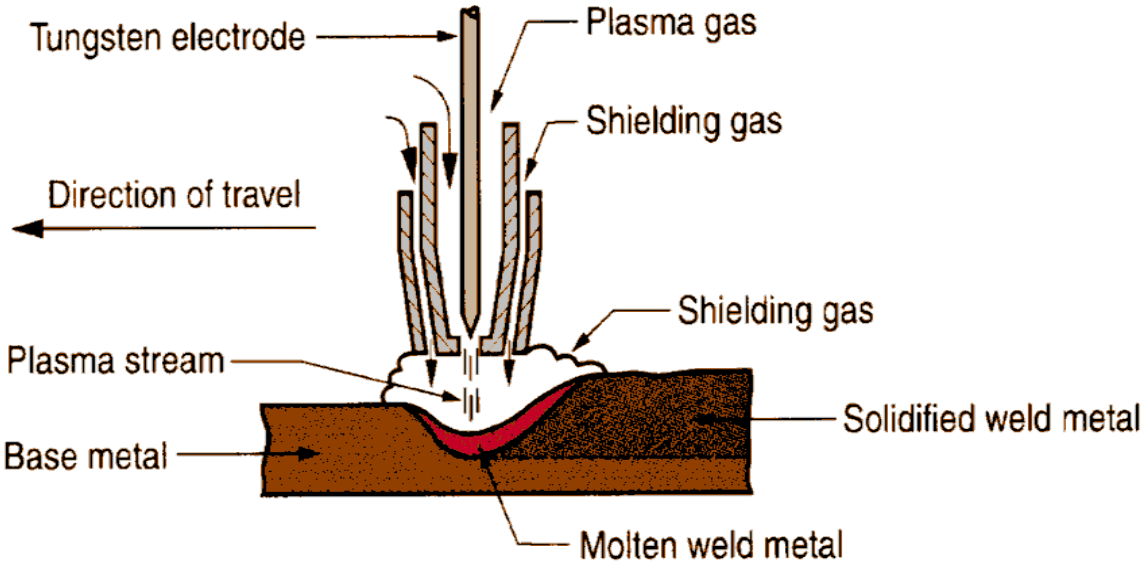

Fig.1 Plasma arc welding [1]

Advantages of plasma arc welding are, it is a high welding speed and High energy available for welding. It can be easily used to weld hard and thick work pieces.During arc formation there is no effect on distance between tool and work piece and Low power consumption for same size weld.The disadvantages of PAW comprise high cost of equipment and larger torch sizes than other arc welding methods [2]. The plasma arc welding processes are widely used in aerospace industries, automation and marine industries for accurate results.

Experimental Procedure

Titanium (Ti-6Al-4V) sheets of 200 x 200 x 0.5 mm are welded autogenously with square butt joint without edge preparation. The chemical composition and tensile properties of Titanium (Ti-6Al-4V) sheet is given in Table 1 & 2

Table:-1 Chemical composition of Titanium (Ti-6Al-4V) (weight %)

V	Al	Fe	C	N	H	O	Ti
5.8	4.00	0.20	0.05	0.03	0.011	0.19	89.71

Table 2 Mechanical properties of Titanium (Ti-6Al-4V)

Young's Modulus	113.8 Gpa
Poison's Ratio	0.342
Tensile yield strength	830 Mpa
Ultimate compressive Strength	1080 Mpa
Ultimate Tensile Strength	900 Mpa
Density	$4.42 g.cm^{-3}$
Thermal conductivity	6.7 W/m-K

High purity argon gas (99.99%) is used as a shielding gas and a trailing gas right after welding to prevent absorption of oxygen and nitrogen from the atmosphere. The welding has been carried out under the welding conditions presented in Table 3.

Table 3 Welding conditions [2]

Power source	Secheron Micro Plasma Arc Machine (Model: PLASMAFIX 50E)
Polarity	DCEN
Mode of operation	Pulse mode
Electrode	2% thoriated tungsten electrode
Electrode Diameter	1 mm
Plasma gas	Argon & Hydrogen
Plasma gas flow rate	6 Lpm
Shielding gas	Argon
Shielding gas flow rate	0.6 Lpm
Purging gas	Argon
Purging gas flow rate	0.6 Lpm
Copper Nozzle diameter	1mm
Nozzle to plate distance	1mm
Welding speed	260 mm/min
Torch Position	Vertical
Operation type	Automatic

There are many influential process parameters which effect the weld quality characteristics of Pulsed Current MPAW process like peak current, back current, pulse rate, pulse width, flow rate of shielding gas, flow rate of purging gas, flow rate of plasma gas, welding speed etc. From the earlier works [3, 21] carried out on Pulsed Current MPAW it was understood that the peak current, back current, pulse rate and pulse width are the dominating parameters which affect the weld quality characteristics. The values of process parameters used in this study are the optimal values obtained from our earlier papers [3,21]. Details about experimental setup are shown in Figure 2

.

a) Welding fixture

b) Power source

c) Plasma and Shielding gas cylinders

Fig.2 MPAW Setup with accessories [3]

Microstructure Analysis

Three metallurgical samples are cut from each joint leaving the edges of defective portion of the welded length. Defective length of weld is identified visually and also by conducting dyes penetrant and X-ray tests and mounted using Bakelite. Sample preparation and mounting is done as per ASTM E 3-1 standard. The transverse face of the samples are surface ground using 120 grit size belt with the help of belt grinder and polished sequentially using grade 1/0 (245 mesh size), grade 2/0(425 mesh size) and grade 3/0 (515 mesh size) sand paper. The specimens are further polished using aluminum oxide, diamond paste and velvet cloth on a disc polishing machine.[5] The polished specimens are macro-etched using Kroll's reagent (100 ml water, 1-3 ml hydrofluoric acid, 2-6 ml nitric acid)solution to reveal the microstructure.

The weld pool geometries were measured at 100X magnification using Inverted Trinocular Metallurgical Microscope, Make: BS Pyromantic, Model No. BSPIL-MET-01013. Weld bead geometry for sample is presented in Figure.3 and Figure.4

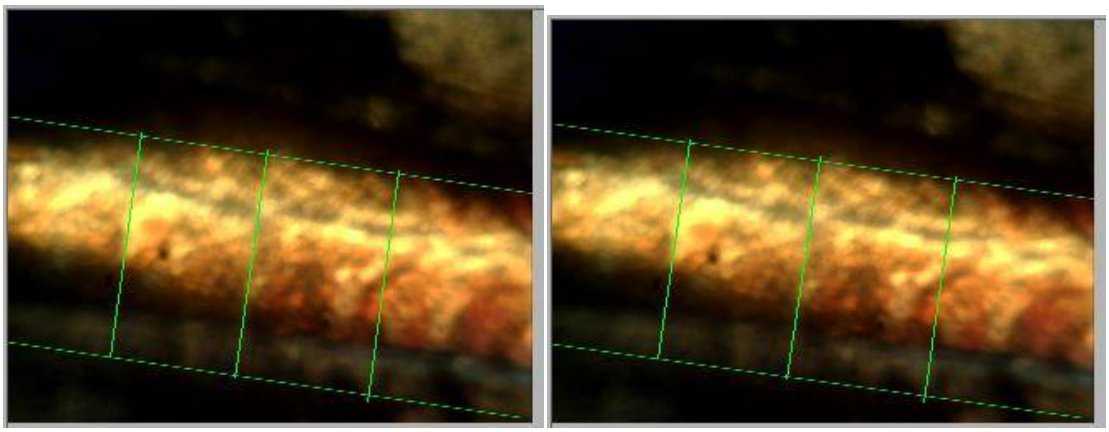

Front width ***Back width***

Fig.3 Weld bead geometry (Before polishing etching) at 100X

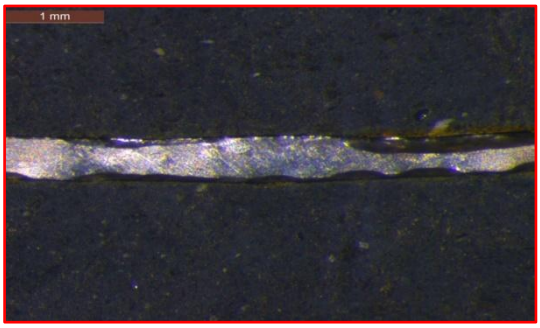

Fig.4 Weld bead geometry after etching at 30X

The experiments were conducted as per the Table.4and the values of weld bead geometry measured by metallurgical microscopes are presented

Table.4 Experimental Results

	INPUT PARAMETERS				**OUTPUT RESPONSES**	
Exp No.	**Peak Current (PC) (Amperes)**	**Base current (BC) (Amperes)**	**Pulse Rate (PR) (Pulses/second)**	**Pulse width (PW) (%)**	**Front Width (mm)**	**Back Width (mm)**
1.	26	11	10	20	1.542	1.4032
2.	**28**	17	50	30	1.563	1.4036
3.	**30**	17	10	40	1.536	1.4031
4.	**32**	11	40	30	1.546	1.4150
5	**34**	15	20	20	1.523	1.3870

FINITE ELEMENT ANALYSIS

Finite element method is one of the most useful methods for calculating the desired values like stress. Strain, deformation, velocity and temperatures. The finite element method in the software name ANSYS (analytical systems).The ANSYS computer program is a large-scale multi-purpose finite program which may be used for solving several classes of engineering analyses. In this software several types' modules are there such as static structural, transient, CFD, study state thermal analysis etc. In this paper we are used in the Ansys module is study state thermal analysis.

Analytical Modeling

The regular method of arriving at welding parameters through experimental trials may not be suitable for titanium (Ti-6Al-4V) alloys because of titanium alloys are high cost. Modeling may be a better alternative to predict the temperature distribution and weld bead shapes and sizes during welding. An analytical model that is capable of providing closed form solutions will be a better alternative to predict the results, which in turns the weld bead geometry. The following assumptions are considered in deriving the analytical solution:

1. The initial temperature of the work piece is 300 K.

2. The plasma arc is traveling with constant velocity along the weld bead.

3. The phase change phenomenon is incorporated by considering the enthalpy of the material.[15]

For any analysis 3 steps are following those are modeling, boundary conditions and solutions. In this paper the modeling is done in Ansys design modular and properties of Ti-6Al-4V such as density 4.42 g/cc, thermal conductivity 6.7 W/m-K , specific heat 0.5263 J/g-c. thesize of the weld bed plate was 200*150*5 mm. simulation of Ti-6Al-4V was done by ANSYS 15.0: the engineering data was selected for Ti-6Al-4V.

Meshing is one of most important part of analysis. It is directly affected the results of simulation. Sometimes results may deviate a little due to meshing. For better results meshing should be dense near to the welding line and rare away from the center line. In this paper we use simple meshing in the size of 2mm as shown in figure 5.

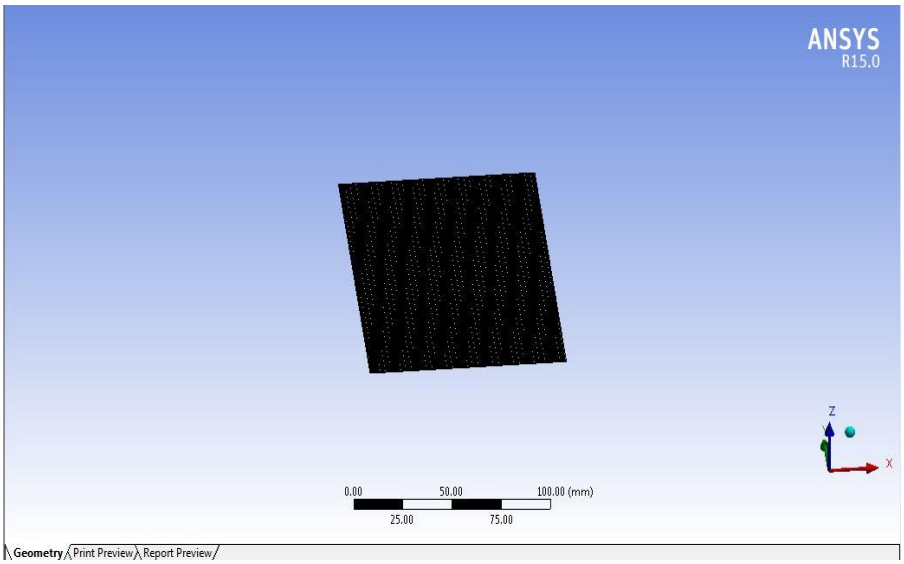

Fig.5 simple meshing on weld bead plate.

After that loading is applied on weld bead plate and the type of loading is thermal loading. Input parameter of this analysis is heat flux. The heat fluxes are loads at 28.86 (W/mm^2), 30.09 (W/mm^2), 27.88 (W/mm^2), 28.95 (W/mm^2) and 28.73 (W/mm^2) are shown in figure 6.

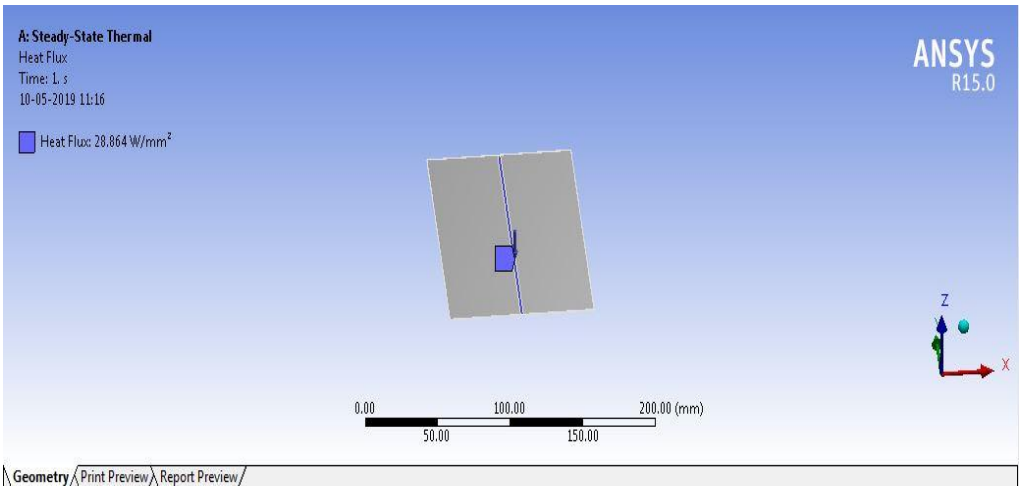

Fig.6 Thermal load on weld bead zone.

Calculation of the heat flux values based on experimental input parameters

Heat flux, $q = -k*\Delta T/\Delta X$

$\Delta T = Q*R$

$V = IR$

$R = V/I$

$Q = VI/N$

ΔX For Weld Bead Plate $= 0.002$ mm

$R = 23/26$

$= 0.884$

$\Delta T = 2.04*0.884$

$= 1.80$

$q = 32*1.80/0.002$

$= 28800/1000$

$= 28.86$ W/ mm^2

Nomenclature; K- thermal conductivity

ΔT- temperature difference

Q - Heat input

V - Voltage in V

I – current in Amps

R – Resistance

N – Welding Speed.

By using this analysis we find out weld bead front and back widths are measured and those values are as shown in figures 7, 8,9,10 and 11 & table.5.

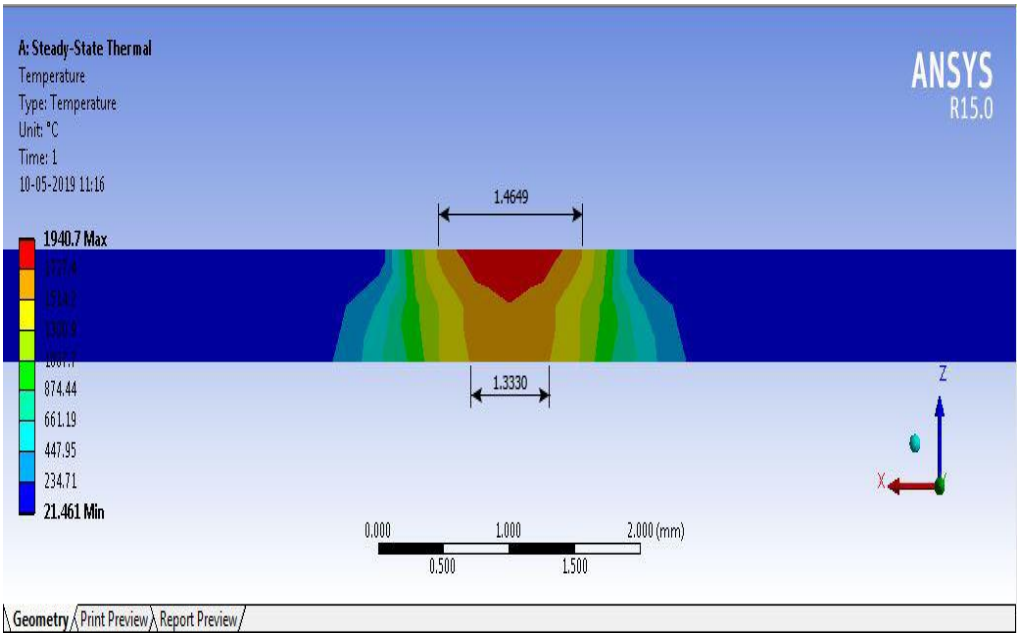

Fig.7 weld bead front width and back width at 28.87 w/mm2

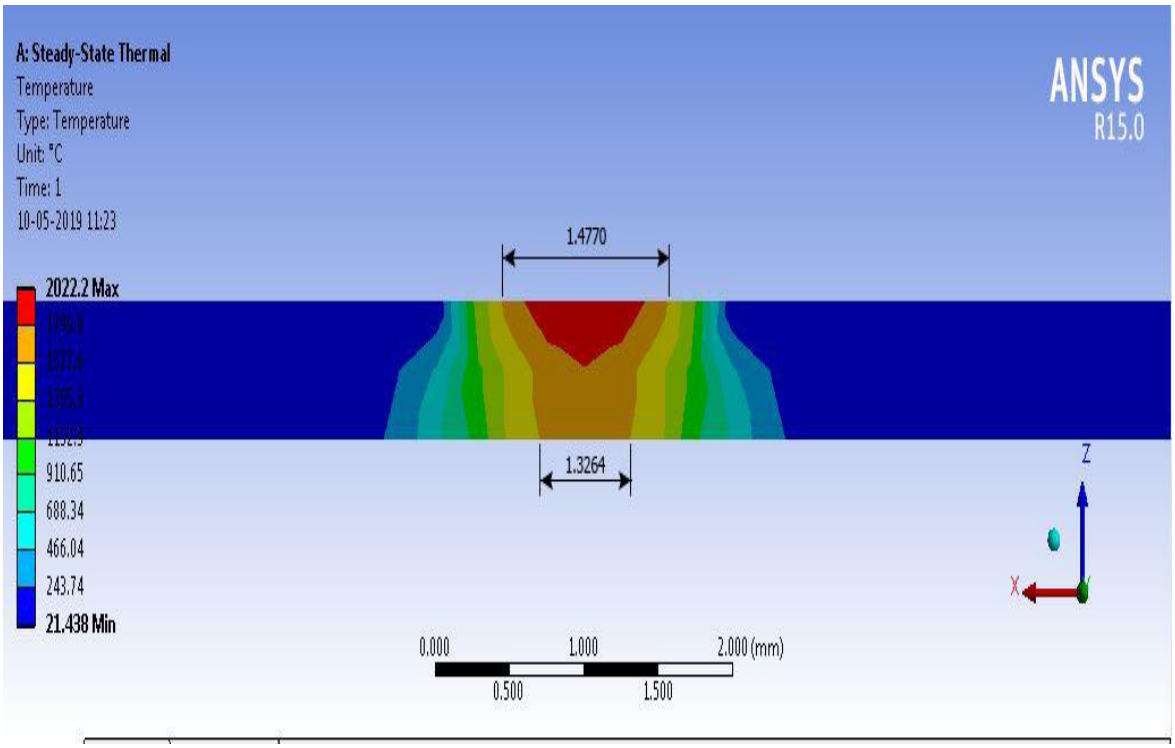

Fig.8 weld bead front width and back width at 30.09 w/mm2

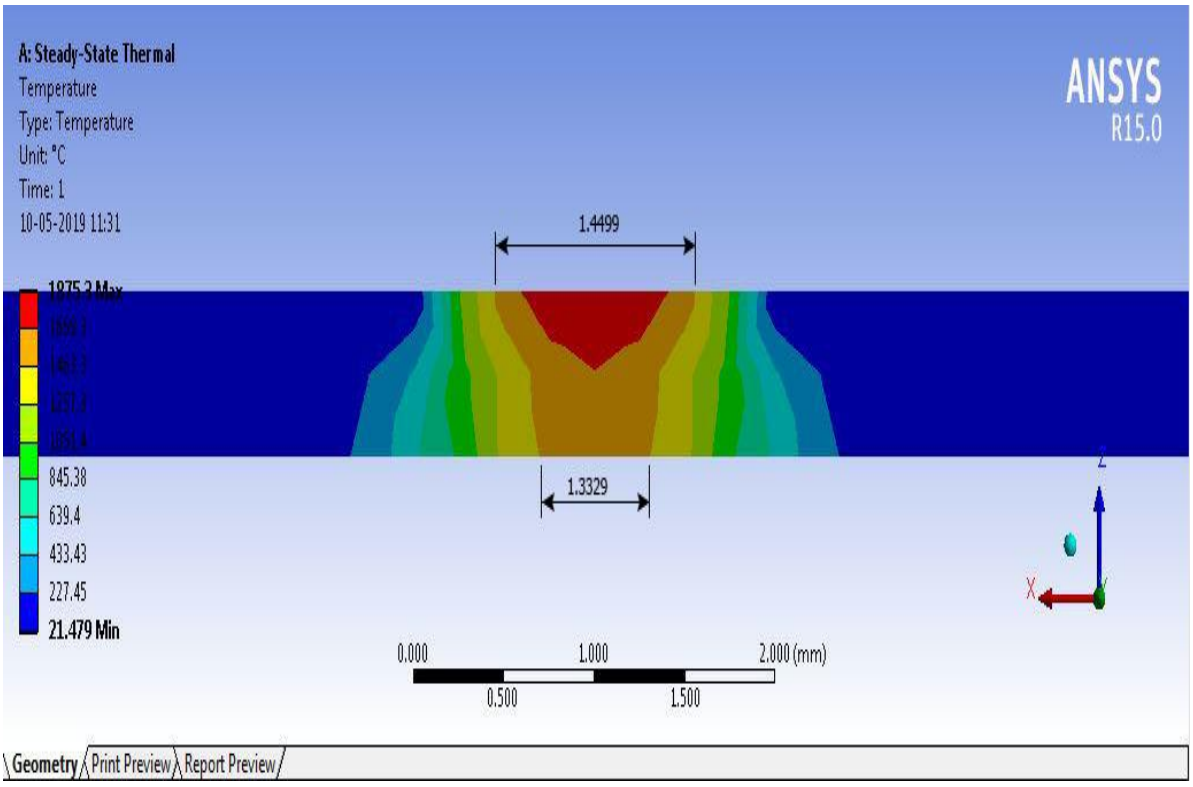

Fig.9 weld bead front width and back width at 28.75 w/mm2

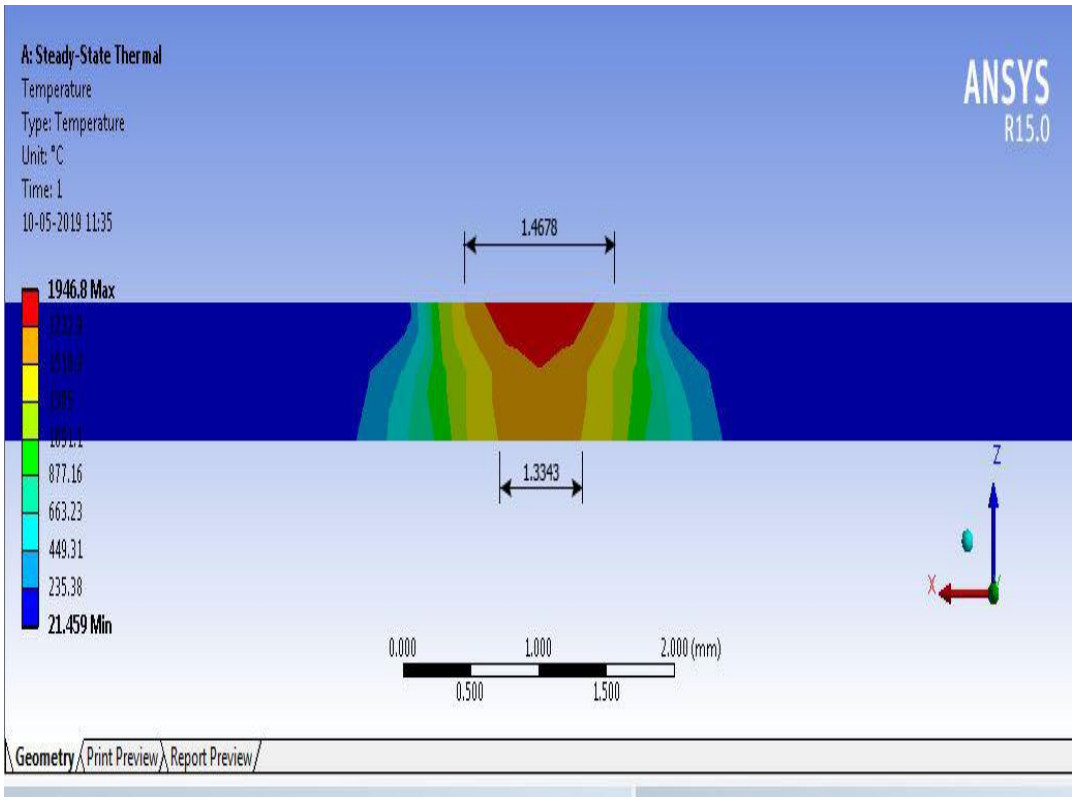

Fig.10 weld bead front width and back width at 28.95 w/mm2.

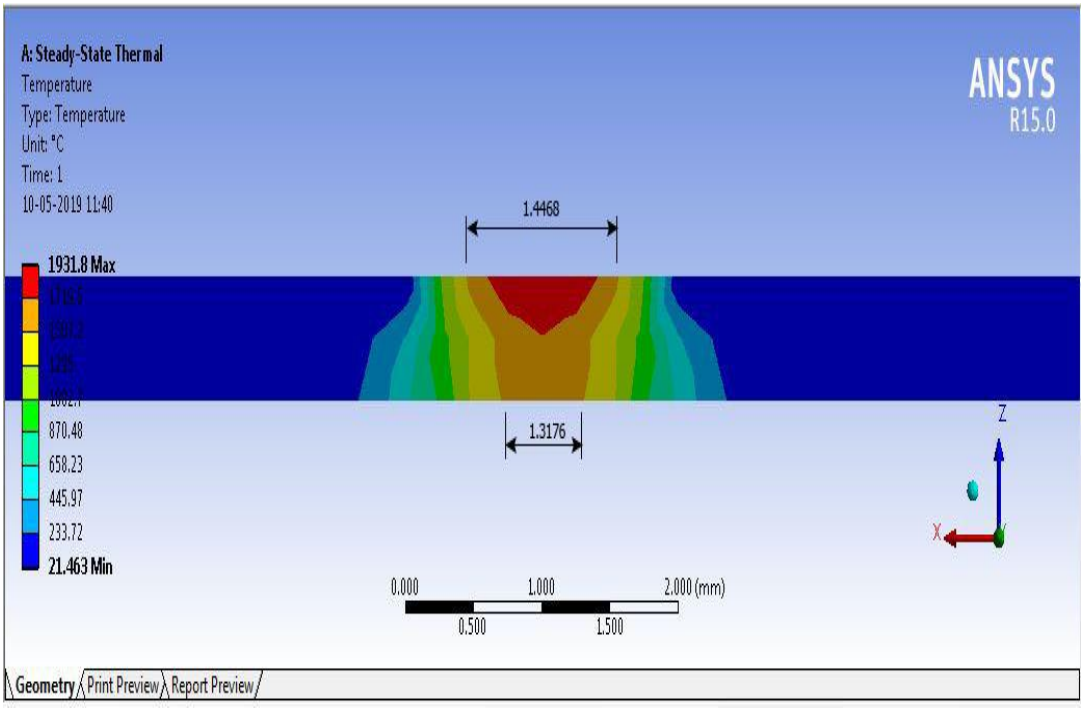

Fig.11 weld bead front width and back width at 28.73 w/mm2

Table.5 Analytical Values

S.No	Heat Flux (W/mm^2)	Front Width (mm)	Back Width (mm)
1.	27.87	1.4649	1.3330
2.	30.09	1.4770	1.3264
3.	28.75	1.4499	1.3329
4.	28.95	1.4678	1.3343
5.	28.73	1.4468	1.3176

RESULTS AND DISCUSSION

Comparison of experimental and FEA values of fronth width and back width are presented in Table.6 and their variation is shown in figures.12 and 13.

Table 6 comparisons of experimental and analytical values

S.no	Exp no	Experimental values		Analytical values	
		Front width	Back width	Front width	Back width
1.	1.	1.5420	1.4032	1.4649	1.3330
2.	10	1.5630	1.4036	1.4770	1.3264
3.	14	1.5360	1.4031	1.4499	1.3329
4.	16	1.5460	1.4150	1.4678	1.3343
5.	23	1.5230	1.3870	1.4468	1.3176

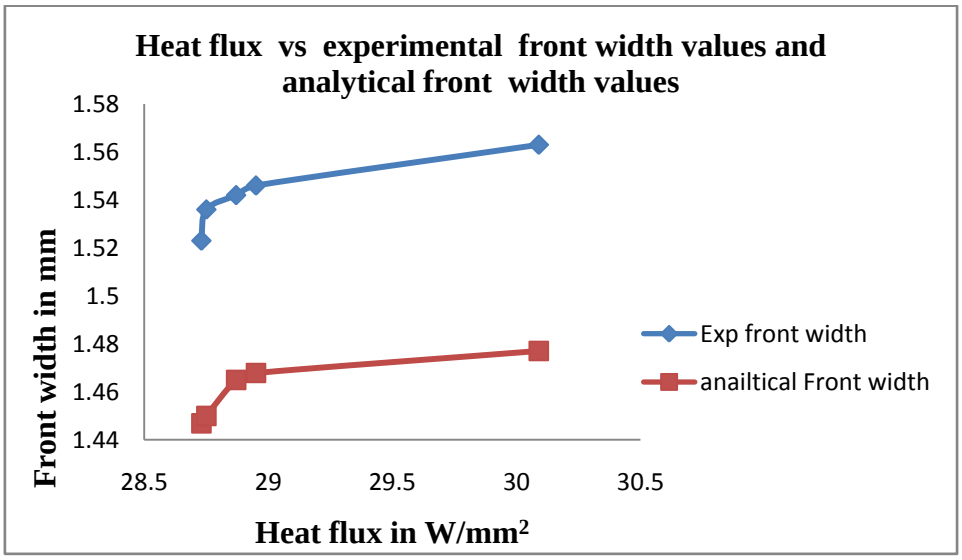

Fig.12 Experimental front width and analytical front width

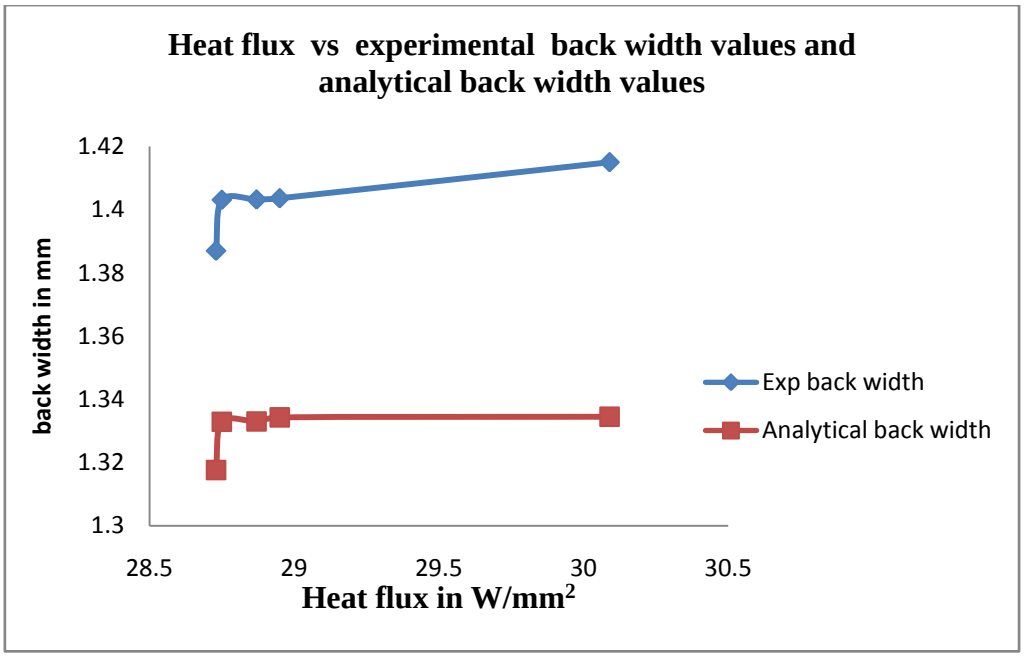

Fig.13 Experimental back width and analytical back width

In optimization processUnderstood that 25 experiments, 21 has the optimal solution. That is at Peak Current of 34 Amps, Base Current of 11 Amps, Pulse rate of 50 Pulses/sec and pulse width of 50 % we get the optimal output (weld bead geometry). As well as analytical process also optimal solution appeared in same condition.

The percentage error between experimental values and analytical values as shown in table 7.

Table.7 % of error

S.no	Exp no	Experimental normalized values		Analytical values		Front width % of error	Back width % of error
		Front width (mm)	Back width (mm)	Front width (mm)	Back width (mm)		
1.	1	1.5420	1.4032	1.4649	1.3330	5.000	5.002
2.	10	1.5630	1.4036	1.4770	1.3264	5.500	5.500
3.	14	1.5360	1.4031	1.4499	1.3329	5.610	5.003
4.	16	1.5460	1.4150	1.4678	1.3343	5.050	5.703
5.	23	1.5230	1.3870	1.4468	1.3176	5.003	5.003

Front width average % error is found to be 5.260, Back width average % error is found to be 5.242 and the very reason for having a margin of 5.260, 5.242 % error with the experimental and Ansys results is due to the series of assumptions that are followed in the experimental values for which exact analytical solution is very difficult process.

CONCLUSIONS

The following conclusions are drawn based on the experiments performed.

- From the experimental and FEA analysis it is understood that front width is large than back width.

- From the experimental FEA analysis it is found that as the peak current increases the front and back width values increases, it is due to large heat inputs at higher currents leading to more melting of the base metal.

- The % error between experimental and FEA values is around 5.2%, this is due to the series of assumptions that are followed in the experimental values for which exact analytical solution is very difficult process.

REFERENCES

I. F. García-Vázquez, A. Aguirre, A. Arizmendi, H. M. Hernández García , L. Santiago-Bautista, J. Acevedo and B. Vargas-Arista,. Analysis of weld bead parameters of overlay deposited on D2 steel components by plasma transferred arc (PTA) process. Materials Science Forum Vol. 755 2013,pp 39-45.

II. V. Dhinakaran, SurajKhope, N. Siva Shanmugam& K.Sankaranarayanasamy ,Numerical Prediction of Weld Bead Geometry in Plasma Arc Welding of Titanium Sheets Using COMSOL. Department of Mechanical Engineering, National Institute of Technology, 2014.

III. V Dhinakaran, N Siva Shanmugam and K Sankaranarayanasamy,. Experimental investigation and numerical simulation of weld bead geometry and temperature distribution during plasma arc welding of thin Ti-6Al-4V sheets2016. Department of Mechanical Engineering, National Institute of Technology.

IV. Guillermo Alvarez Bustard, SadekCriso ´stomoAbsi Alfaro. Measurement and estimation of the weld bead geometry in arc welding processes: the last 50 years of development; Journal of the Brazilian Society of Mechanical Sciences and Engineering 201840:444.

V. Pei-Quan Xu, Leijun Li, Chunbo (Sam) Zhang , Microstructure characterization of laser welded Ti-6Al-4V fusion zones, material characterization 8 7 (2 0 1 4), pp 1 7 9– 185.

VI. Chandan Kumara, ManasDasa, C.P. Paul, K.S. Bindra , Comparison of bead shape, microstructure and mechanical properties of fiber laser beam welding of 2 mm thick plates of Ti-6Al-4V alloy, Optics and Laser Technology 105 (2018), pp 306–321.

VII. K. DevendraNathRamkumar, Vinayak Varma, Madhukar Prasad, N. Deva Rajan, N. Siva Shanmugam,Effectofactivatedfluxo n penetration depth,microstructure andmechanical properties of Ti-6Al-4V TIG welds, journal of material processing tech 261 (2018), pp 233-241.

VIII. Y.Y. Sun , P. Wang, S.L. Lu , L.Q. Li , M.L.S. Nai, J. Wela,Laser welding of electron beam melted Ti-6Al-4V to wrought Ti-6Al4V, Effect of welding angle on microstructure and mechanical properties,Journal of Alloys and Compounds 782 (2019), pp 967-972.

IX. Kamlesh Kumar, ManojMasanta, Santosh Kumar Sahoo, Microstructure evolution and metallurgical characteristic of bead-onplate TIG welding of Ti-6Al-4V alloy, Journal of Materials Processing Tech. (2018).

X. Ali Khurram, Majid Ghomeshi, Mohammad Reza SoleymaniYazdi, Mahmood Moradi , Optimization of Bead Geometry in CO2 Laser Welding of Ti 6Al 4V Using Response Surface Methodology; Engineering, 2011, 3, pp708-712.

XI. Pawan Kumar, Kishore p. Kolhe, Prakash r. Kolhe and c.k. datta, Optimizing pulsed GTAW process

parameters for bead geometry of titanium alloy using taguchi method,Asian Sciences (June & December, 2009) Vol. 4 Issue 1 & 2 , pp 78-82.

XII. Abhishek B P, Anil Kumar G,Madhusudhan.T, Experimental And Finite Element Analysis Of Thermally Induced Residual Stresses For Stainless Steel 303gradeUsing Gmaw Process, International Research Journal of EngineeringTechnology (IRJET),Volume: 02 Issue: 02 | May-2015.

XIII. Edwin Raja Dhas, J.a and Somasundaram, K, Modeling and prediction of HAZ usingfinite element and neural network modeling, Advances in Production Engineering &Management, Volume 8 Number1 March2013,pp 13–24.

XIV. V Dhinakaran, N Siva Shanmugam and K Sankaranarayanasamy, Some studies on temperature field during plasma arc welding of thin titanium alloy sheets using parabolic Gaussian heat source model 2015, Mechanical Engineering Science,pp 1–17.

XV. C.S. Wu, Q.X. Hu, J.Q. Gao, An adaptive heat source model for finite-element analysis of keyhole plasma arc welding; Computational Materials Science 46 2009, pp 167–172.

XVI. Prashant Sagar, Deepak Kumar Gope and SomnathChattopadhyaya. Thermal analysis of TIG welded Ti-6Al-4V plates using ANSYS 2018, International Conference on Mechanical, Materials and Renewable Energy, 377-012113.

XVII. Sadaf Batool, Mushtaq Khan et al, Analysis of weld characteristics of microplasma arc welding and tungsten inert gas welding of thin stainless steel 304L sheet 2015, Design and Applications, 10.1177.

XVIII. Tao Zhang, Chuan Song Wu, and Yanhui Feng,. Numerical analysis of heat transfer and fluid flow in keyhole plasma arc welding 2013, MOE Key Lab for Liquid–Solid Structure Evolution and Materials Processing, Institute of Materials

Joining, Shandong University, Jinan, P. R. China, pp 1521-0634 .

XIX. Hafiz Waqar Ahmad , Jeong Ho Hwang, Ju Hwa Lee and Dong Ho Bae .Welding Residual Stress Analysis and Fatigue Strength Assessment of Multi-Pass Dissimilar Material Welded Joint between Alloy 617 and 12Cr Steel 2017, Graduate School of Mechanical Engineering, Sungkyunkwan University, Suwon , pp 440-746.

XX. HarinadhVemanaboina , G. Edison , Suresh Akella, Distortion control in multi pass dissimilar GTAW process using Taguchi ANOVA analysis , International Journal of Engineering & Technology, 7 (3) 2018, pp 1140-1144.

XXI. Langford G. Plasma arc welding for large titanium aerospace structures. SAE technical paper 660646, 1966.

XXII. Martikainen JK and Moisio TJI. Investigation of the effect of welding parameters on weld quality of plasma arc keyhole welding of structural steels. Weld Res Suppl 1993, 2(7), pp 329s–340s.

XXIII. Boyer R, Welsch, G and Coolings EW. Material properties handbook: titanium alloys. Materials Park, OH: ASM International, 2007.

XXIV. E. Grundy's and S. Meskinis, Influence of Plasma Transferred Arc Process Parameters on Structure and Mechanical Properties of Wear Resistive NiCrBSi-WC/Co Coatings, Materials Science 17 (2011), pp 140-144.

XXV. https://www.usgs.gov/centers/nmic/titanium-statistics-and-information.

XXVI. https://www.wisegeek.com/what-is-a-bead-weld.htm.

XXVII. B. Howard, Surfacing for wear resistance, Stephen Helba et al. (eds.), Modern Welding Technology, Prentice Hall Inc., New Jersey 2002, pp 721-726.

XXVIII. Langford G. Plasma arc welding for large titanium aerospace

structures. SAE technical paper 660646, 1966.

XXIX. Filip R, Kubiak K, Ziaja W, Sieniawski J. The effect of microstructure on the mechanical properties of two-phase titanium alloys. J Mater Process Technol 2003; 133:84–9.

XXX. Ahmadi, E., Ebrahimi, A.R., 2015. Welding of 316L austenitic stainless steel with activated tungsten inert gas process. J. Mater. Eng. Perform. 24, pp 1065–1071.

XXXI. M. J. Donachie, "Titanium: A Technical Guide," American Society for Microbiology International, Materials Park, 1988, pp133-156.

XXXII. A. A. Mohamed, "Optimization of Weld Bead Dimensions in GTAW of Al-Mg Alloy," Materials and Manufacturing Processes, Vol. 16, No. 5, 2001, pp725-736.

XXXIII. Lu F, Tang X, Yu H and Yao S 2006 Numerical simulation on interaction between TIG welding arc and weld pool Compute. Mater. Sci. 35, pp 458–65.

XXXIV. Phillip J Ross, Taguchi Techniques for Quality Engineering, Tata McGraw Hill, 2008.

XXXV. Hugo I. Medellín-Castillo & Dirk F. de Lange & Fernando Ramírez-Cardona & Pedro de J. Garcia-Zugasti., Weld quality analysis and evaluation of plasma arc welds in electrical stators. Int J Adv Manu Technology 2013 64, pp 737–747.

Cite this Article As

Posimsetti Hanuma, Dr. Kondapalli Siva Prasad (2019**). Finite Element Analysis of Weld Bead Geometry of Micro Plasma Arc Welding Titanium (Ti-6al-4v) Alloy** Journal of Material Science & Manufacturing Technology, 4(2), 38- 57

http://doi.org/10.5281/zenodo.3373127